Tumor Biol.
DOI 10.1007/s13277-015-3314-5

RESEARCH ARTICLE

A Huaier polysaccharide reduced metastasis of human hepatocellular carcinoma SMMC-7721 cells via modulating AUF-1 signaling pathway

Cong Li · Xia Wu · Honghai Zhang · Gengxia Yang · Meijun Hao · Shoupeng Sheng · Yu Sun · Jiang Long · Caixia Hu · Xicai Sun · Li Li · Jiasheng Zheng

Received: 22 February 2015 / Accepted: 5 March 2015

Abstract TP-1 is a polysaccharide from one famous fungus Huaier. Treatment with TP-1 significantly inhibited the cell growth, adhesion, migration, and motility of SMMC-7721 cells in a dose-dependent manner. Real-time quantitative RT-PCR revealed a dose-dependent decrease in RNA-binding factor 1 (AUF-1) and astrocyte elevated gene-1 (AEG-1) messenger RNA (mRNA) levels in TP-1-treated SMMC-7721 cells, which is consistent with their protein expression detected by Western blotting. On the contrary, microRNA-122 (miR-122) expression increased in SMMC-7721 cells following TP-1 treatment. Moreover, TP-1 treatment at three doses apparently increased epithelial marker E-cadherin protein expression but decreased the mesenchymal marker N-cadherin protein level. In addition, the hematoxylin-eosin (H & E) staining showed that the TP-1 significantly inhibited the lung metastasis of liver cancer in mice orthotopic implanted with SMMC-7721 tumor tissue. Taken together, these findings proved the inhibitory effect of TP-1 on the growth and metastasis of SMMC-7721 cells, and TP-1 might be offered for future application as a powerful chemopreventive agent against hepatocellular carcinoma (HCC) metastasis.

Keywords Huaier polysaccharide · Metastasis · Hepatocellular carcinoma · RNA-binding factor 1 (AUF-1) · Astrocyte elevated gene-1 (AEG-1) · Epithelial-mesenchymal transition (EMT)

Introduction

Hepatocellular carcinoma (HCC) is one of the most common malignant tumors that threats global public health and a leading cause of cancer-related mortality throughout the world [1]. The mortality of more than 90 % of cancer patients is not due to their primary tumors but to the development of invasiveness and metastases [2]. Until now, systemic treatment of human HCC has not been effective in most cases, and its clinical therapy is a major challenge. Therefore, an effective method of blockading the advancement of HCC and reducing mortality is to inhibit its invasion and metastasis.

Metastasis, a hallmark of malignancy, is a complex phenomenon in which tumor cells detached from the primary neoplasm invade to distant sites to form secondary tumors [3]. This metastatic process comprises a cascade of events including cancer cell adhesion, invasion, migration, circulation in blood and lymph, as well as proliferation at a target site [4]. It is the principal cause of mortality among cancer patients, and to date, no therapeutic option is available. Thus, it is critical to develop effective antimetastatic agents. However, the process and causes of metastasis are very complicated. This process is

Cong Li and Xia Wu contributed equally to this work.

C. Li · H. Zhang · G. Yang · M. Hao · S. Sheng · Y. Sun · J. Long · C. Hu · J. Zheng (✉)
Intervention Therapy Center of Liver Diseases, Beijing You An Hospital, Capital Medical University, 100069 Beijing, China
e-mail: jiashengzheng@outlook.com

X. Wu
Department of Infectious Disease, the Second Affiliated Hospital of Harbin Medical University, 150081 Harbin, China

X. Sun
School of Medicine, Tsinghua Center for Life Sciences, Tsinghua University, 100084 Beijing, China

L. Li
Institute of Liver Diseases, Beijing You An Hospital, Capital Medical University, 100069 Beijing, China

Published online: 19 March 2015

greatly dependent on the expression of key proteases, their inhibitory proteins, the signaling pathways that control them, and surrounding host factors such as host resistance to cancerous cells. In a previous study, we demonstrated that high RNA-binding factor 1 (AUF-1) expression in 146 HCC patients was closely associated with tumor size, suggesting that the AUF-1 gene may play an important role in HCC progression and be a novel biomarker in the future [5]. We also find that the astrocyte elevated gene-1 (AEG-1) was overexpressed in HCC tissues from 144 patients and epithelial-mesenchymal transition (EMT) appeared in these tumor tissues, which is a critical process in cancer development, enhancing cancer cells' ability to metastasize [6]. In addition, microRNA-122 (miR-122), a tumor suppressor against HCC, is frequently observed with a low expression in HCC and is closely related to poor differentiation, larger tumor size, metastasis and invasion, and poor prognosis [7]. Therefore, an antimetastasis drug from a natural source that inhibits or suppresses the expression of AUF-1, AEG-1, and EMT, but increases miR-122 level, would be of great clinical value to prevent hepatocarcinogenesis and the invasion of HCC. As expected, our preliminary data have proven that crude Huaier polysaccharides could effectively inhibit the proliferation, adhesion, migration, and invasion of HCC cells in vitro, at least in part, by repressing AEG-1 and EMT expression [8]. To build on these previous findings, the current study objective was to determine the effect of one purified Huaier polysaccharide on the metastasis of HCC cells in vitro and further explore the underlying mechanism for the involvement of AUF-1, AEG-1, miR-122, and EMT in tumor cell invasion and metastasis. Furthermore, we also investigated whether this polysaccharide could inhibit tumor cell metastasis in an in vivo model.

Materials and methods

Materials and chemicals

Huaier extract was donated by Qidong Gaitianli Pharmaceutical Co., Ltd. (Jiangsu, China). 3-(4,5-Dimethylthiazol-2-yl)-2,5-diphenyltetrazolium bromide (MTT), trifluoroacetic acid (TFA), standard sugars, bovine serum albumin (BSA), and dimethyl sulfoxide (DMSO) were purchased from Sigma Chemical Co. (St. Louis, MO, USA). Fetal calf serum (FCS) and Dulbecco's modified Eagle's medium (DMEM) were purchased from Gibco Invitrogen Co. (Grand Island, NY, USA). DEAE-cellulose-52 and Sepharose CL-6B were from Amersham (Sweden). All other chemicals were of the highest commercial grade available.

Isolation and purification of Huaier polysaccharides

Dried sample (500 g) was defatted with 95 % ethanol under reflux twice at 80 °C for 2 h, to remove colored materials, monosaccharides, oligosaccharides, and small molecule materials. The residue was then extracted with 10 L of boiling water three times for 2 h for each time. After centrifugation (1700×*g* for 15 min), the supernatant was concentrated in a rotary evaporator under reduced pressure to a final concentration of 8 % (*m*/*v*), after which a three-fifth volume of Sevage reagent was added to remove the protein for five times [9], and then exhaustively dialyzed against water for 2 days. Then, the concentrated dialysate was precipitated by the addition of 95 % ethanol to a final concentration of 40 % (*v*/*v*) for 24 h at 4 °C. The precipitates collected by centrifugation (3000×*g* for 10 min, at 20 °C) were washed with absolute ethanol, acetone, and ether, respectively, to yield the crude polysaccharide, named as TCP-40.

The TCP-40 was dissolved in distilled water and filtered through a 0.45-μm Millipore membrane, and the resulting concentrated dialysate was applied to a column of DEAE-cellulose-52 (2.6 cm×30 cm) equilibrated with deionized water. After loading with the sample, the column was eluted with stepwise NaCl aqueous solution (0.1 and 0.5 M, pH 6–7) at a flow rate of 2 mL/min. Each fraction was collected using an automated step-by-step fraction collector and monitored with the phenol-sulfuric acid method at 490 nm absorbance for polysaccharides. Two fractions eluted by 0.1 and 0.5 M NaCl solution were collected, dialyzed, and lyophilized. The fraction (TCP-40-1) eluted with 0.1 M NaCl was further fractioned on a Sepharose CL-6B column (2.6×100 cm) eluted with 0.15 M NaCl at a flow rate of 1 mL/min to yield one purified polysaccharide, named as TP-1.

Molecular weight determination

The average molecular weight of TP-1 was determined by high-performance size-exclusion chromatography (HPSEC), which was performed on a Waters UPLC system equipped with a TSK-G3000 PWXL column (7.8 mm ID×30.0 cm) and a RID detector. The mobile phase was deionized water, and the flow rate was 0.3 mL/min at 30 °C. The sample (2.0 mg) was dissolved in distilled water (2 mL) and passed through a 0.45-μm filter and 20 μL of the supernatant was injected after centrifuged (8000 rpm; 3 min). The molecular mass was estimated by reference to a calibration curve made from various T-series dextran standards (T-2000, T-1000, T-500, T-100, and T-50, T-20, T-10) using linear regression.

Monosaccharide composition and chemical properties

Gas chromatography (GC) was used for identification and quantification of the monosaccharides. Briefly, TP-1 (10 mg) was hydrolyzed in 1 mL of 2 M TFA at 100 °C for 2 h. Then, the monosaccharides were conventionally converted into the alditol acetates as described by Tian et al. [10] and were analyzed by GC. Standard monosaccharides (L-rhamnose, D-

arabinose, D-xylose, D-mannose, D-glucose, and D-galactose) were also derived and analyzed under the same procedure.

Total carbohydrate and protein of these polysaccharides were determined by the phenol-sulfuric acid assay using D-glucose as the standard [11] and the Bradford method using BSA as the standard [12], respectively. In addition, total uronic acid content was determined by photometry with m-hydroxybiphenyl at 523 nm [13], using GalA as standard.

Cell lines

Human hepatocellular carcinoma SMMC-7721 cell line was obtained from Shanghai Institute of Cell Biology in the Chinese Academy of Sciences and was routinely cultured in DMEM supplemented with 10 % heat-inactivated FCS, 100 U/mL penicillin, 100 μg/mL streptomycin, 1 % sodium pyruvate, and 2 mM L-glutamine at 37 °C in a humidified atmosphere of 5 % CO_2 and 95 % air. The human liver WRL-68 and PCC cell lines (ATCC, Manassas, VA, USA) were grown in 25-cm^2 flasks using DMEM supplemented with 10 % heat-inactivated FCS, 100 U/mL penicillin, 100 μg/mL streptomycin, 2.5 μg/mL fungizone, 2 mM L-glutamine, 20 mU/mL insulin, 50 nM dexamethasone, 50 μg/mL gentamycin, and 100 μg/mL vancomycin at 37 °C in a humidified chamber with 5 % CO_2. The cells were passaged at the estimated log growth phase until a sufficient number of 80–90 % confluent 25-cm^2 flasks were obtained for each experiment.

Cytotoxicity assay

Cell proliferation was assessed using the MTT dye reduction assay [14]. One day before the assay, SMMC-7721 cells were seeded at a density of 1×10^5 cells per well in 96-well flat bottom plates in a culture medium containing 10 % FCS. The next day, the cultures were washed and the cells were treated with various concentrations of TP-1 (0, 25, 50, or 100 μg/mL). After 24 h, 50 μL of MTT (5 mg/mL in PBS) was added to each well and the plates were incubated for an additional 4 h at 37 °C. The medium was discarded and the formazen crystals, which were formed in the cells, were dissolved by the addition of 100 μL DMSO. The optical density of each well was determined using an ELISA plate reader (Molecular Devices, CA, USA) at 570 nm. The inhibition rate was calculated by the formula: inhibition rate of proliferation (%)=$(A_{\text{control}}-A_{\text{treated}})/A_{\text{control}}\times100$ %.

Tumor cell adhesion assay

The cell attachment assay was carried out in 96-well plates using a method described elsewhere [15], with some modifications. Briefly, a 96-well plate was coated with Matrigel (11 mg/mL) and incubated for 2 h. Then, 2 % (0.1 %) BSA was added into each coated well and incubated at 37 °C for 1 h to block any possible unbounded sites. Prior to the addition of the cells to each well, the cells were incubated in DMEM medium containing 10 % heat-inactivated FCS in the presence of TP-1 (25, 50, or 100 μg/mL) or PBS at 37 °C for 30 min. After a further incubation at 37 °C in a humidified incubator for 24 h, the unbound cells were gently washed out and the adhesion cells were measured using the MTT method as we previously described in the "Cytotoxicity assay" section. The adhesion rate was calculated as $A_{\text{experimental group}}/A_{\text{control group}}\times100$ %.

Wound-healing assay

To determine the cell motility, SMMC-7721 cells (1×10^5 cells/mL) were plated in 6-well culture plates and allowed to grow to complete confluence. After being confluenced, a sterile micropipette tip was drawn across the center of the cell monolayer to produce a clean 1-mm-wide wound area. Subsequently, the wounded SMMC-7721 cell layer was washed with fresh medium to remove loose cells and replaced by serum-free medium with or without TP-1 at 25, 50, or 100 μg/mL, respectively. After incubation for 24 h, cell migration was observed and photos were taken under a phase-contrast inverted microscope. The migrated cells across the white lines were counted in five randomly chose fields from each triplicate treatment, and data are presented as the mean±SD.

Transwell chemotaxis migration assay

The spontaneous migration abilities of the SMMC-7721 cells following treatment with various concentrations of TP-1 were performed in Transwell chambers using a polycarbonate filter with an 8-μm pore size in a 24-well plate. For cell invasion assay, the filter membranes were coated with the reconstituted basement membrane Matrigel (50 μg/filter). The SMMC-7721 cells were detached by trypsin from the culture flasks and resuspended at 1.5×10^5 cells/mL in serum-free medium, and then 50 μL cell suspension was seeded to the upper chambers at a density of 1×10^5 cells/well in the absence or presence of various concentrations of TP-1 (25, 50, or 100 μg/mL). Afterwards, the medium containing 10 % FCS was applied to the lower chamber as chemoattractant. Then, the Transwells were incubated at 37 °C for 24 h. At the end of incubation, the cells remaining in the upper surface of the membrane were gently removed with a cotton-tipped swab, and the cells that migrated to the opposite surface of the filter membrane were fixed with methanol and stained with 0.1 % crystal violet. Cells that migrated to the lower surface of the Transwell membrane were counted under a light microscope at five randomly selected fields (×400 magnification). The migration rate was

calculated as [(Migration cells treated/Migration cells control)×100 %].

Western blotting analysis

To analyze the migration-related proteins, the cellular proteins were isolated from SMMC-7721 cells following treatment with TP-1 (25, 50, or 100 μg/mL) for 24 h by the addition of 200 μL of lysis buffer [20 mM Tris pH 7.5, 150 mM NaCl, 1 % Triton X-100, 2.5 mM sodium pyrophosphate, 1 mM EDTA, 1 % Na_3CO_4, 0.5 μg/mL leupeptin, 1 mM phenylmethanesulfonyl fluoride (PMSF)]. Equivalent amounts of protein (30 μg) were separated on 10–12 % SDS-PAGE gels and transferred onto nitrocellulose membranes. Nonspecific binding of the membranes was blocked with Tris-buffered saline (TBS) containing 1 % (*w*/*v*) nonfat dry milk in TBST (20 mM Tris-HCl (pH 7.6), 8.2 g/L NaCl, and 0.1 % Tween 20) for 1 h at room temperature. After blocking, the blots were incubated with primary antibodies against AUF-1, AEG-1, E-cadherin, N-cadherin, and β-actin overnight at 4 °C. The membranes were washed three times with TBST and incubated with appropriate peroxidase-conjugated secondary antibody, and the immunoreactive proteins were detected using an enhanced chemiluminescence kit (Amersham, USA) according to the manufacturer's instructions.

Real-time quantitative RT-PCR

Total RNA was extracted using TRIzol (Invitrogen) according to the product specification, and the concentration of total RNA was checked using a NanoDrop 2000c Spectrophotometer (Thermo Scientific). One microgram of total RNA was taken for RT-PCR with the following cDNA used in a subsequent amplification: miR-122: GGGGTGGAGTGTGACA ATG (sense) and CAGTGCGTGTCGTGGAGT (antisense); AUF-1 messenger RNA (mRNA): AGTGTAGATAAGGT CATGGATC (sense) and CTCTTCCACGAGCTCTTC (antisense); AEG-1 mRNA: ACGACCTGGCCTTGCTGA AGAATCT (sense) and CGGTTGTAAGTTGCTCGGTG GTAA (antisense); U6 small nuclear RNA (U6 small nuclear RNA (snRNA)): GCTTCGGCAGCACATATACTAAAAT (sense) and CGCTTCACGAATTTGCGTGTCAT (antisense); and GAPDH mRNA: AGCCGCATCTTCTTTT GCGTC (sense) and TCATATTTGGCAGGTTTTTCT (antisense). The results for miR-122 were normalized with U6 snRNA that was used as an endogenous control and GAPD H as another internal reference to normalize AUF-1 and AEG-1 mRNA. Amplification was performed in a ABI7300 real-time PCR system (Applied Biosystems, CA) at 95 °C for 10 min, followed by 40 cycles of 95 °C for 31 s and 60 °C for 1 min. The relative quantification of gene expression was analyzed by the $2^{-\Delta\Delta Ct}$ method [16].

Orthotopic murine liver tumor model of distant metastasis

Male athymic BALB/c nu/nu mice were purchased from the Research Center of Laboratory Animals, Harbin Medical University (Harbin, China). All the animals were maintained under standard condition (temperature at 25±2 °C, 12 h dark-light cycle and 60–70 % relative humidity and fed with normal mice chow and water ad libitum). The experiments were carried out in accordance with the ethical principles of the Institutional Ethical Committee of Harbin Medical University for the care and use of laboratory animals.

An orthotopic HCC metastasis tumor model was established using SMMC-7721, which has metastatic potential to the lung [17]. SMMC-7721 cells (2×10^6 cells in 0.1 mL PBS) were injected subcutaneously into the right upper flank region of 4-week-old male Balb/c nude mice to establish subcutaneous xenograft models. When the size reached to about 10 mm^3, the tumors were removed from mice, cut into 1-mm^3 pieces, and implanted into the left lobe of the nude mouse liver to establish orthotopic xenograft models as described previously [18]. Briefly, after a left upper abdominal transverse incision was made under anesthesia, a part of the liver surface on the left lobe of the liver was exposed and mechanically injured with scissors. Next, a tumor block of 0.2 cm× 0.2 cm×0.2 cm was implanted into the left liver tissue, the wounds were closed primarily, and the abdominal wall was closed. After the operation, mice were kept under specific pathogen-free conditions and given free access to mouse chow. Then, all mice bearing orthotopic xenografts were randomly divided into four groups of six mice each and treated with or without TP-1 (200, 400, and 800 μg/kg) via intragastric administration for four consecutive weeks at day 1 after orthotopic implantation. Four weeks later, mice were sacrificed. The lung tissue was fixed in 10 % formalin, embedded in paraffin, and cut into 5 mm slides, and metastatic foci on the lung surface were observed and counted under a light microscope.

Statistical analysis

Data is presented as the mean±SD. Statistical analysis was conducted using Student's *t* test and $P<0.05$ was considered statistically significant using the GraphPad Prism 5.0 software.

Results

Purification and physicochemical properties of TP-1

The water-soluble crude polysaccharides (TCP-40) were obtained from Huaier extract by removing protein, dialysis against water, ethanol precipitation, and drying by solvent

exchange. TCP-40 was further fractioned on an anion-exchange column of DEAE-cellulose-52 using 0.1 and 0.5 M of NaCl aqueous solution as eluant, yielding two homogeneous fractions (Fig. 1a). For more purification, one fraction of TCP-40-1 eluted by 0.1 M NaCl was again purified on Sepharose CL-6B gel permeation chromatography to give a colorless polysaccharide (TP-1, Fig. 1b).

The homogeneity of TP-1 was estimated by HPGPC, in which it showed a single and symmetrically sharp peak at a retention time of around 15.5 min, which was estimated to be about 2.3×10^6 Da by comparing with the dextran standards of different molecular weights (data not shown). Chemical composition analysis indicated that TP-1 contained 93.2 % carbohydrate and was free of proteins and uronic acid. A negative response to the Bradford test and no absorption at 280 or 260 nm in the UV spectrum indicated the absence of protein and nucleic acid. Additionally, GC analysis showed that TP-1 was composed of mannose, galactose, rhamnose, glucose, and arabinose, with molar ratios of 3.1:2.2:2.0:1.1:0.5.

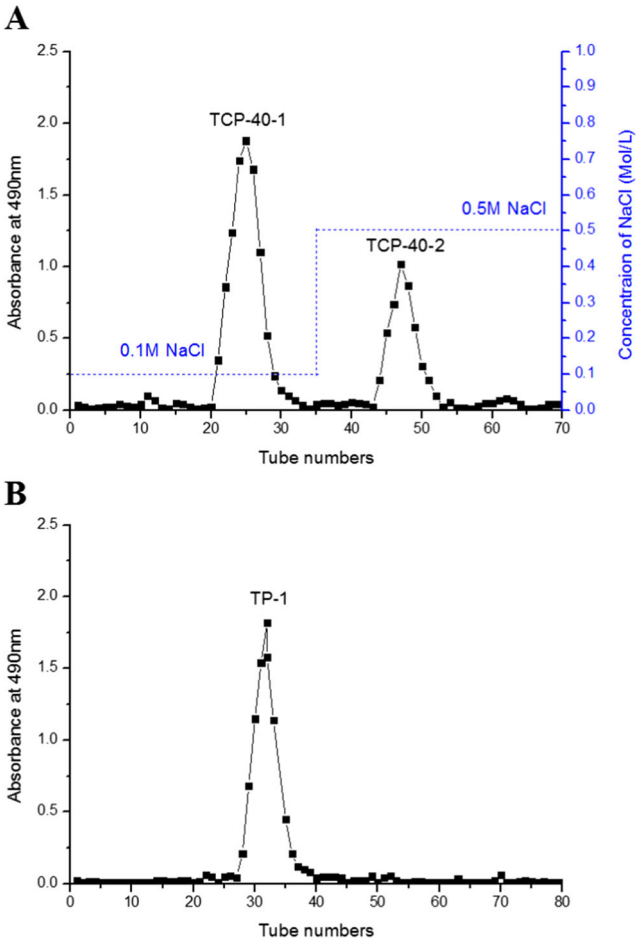

Fig. 1 **a** Elution profiles of the crude polysaccharide TCP-40 from Huaier mushroom on DEAE-cellulose-52 column (2.6 cm×30 cm). **b** Elution profiles of the polysaccharide fraction TCP-40-1 on Sepharose CL-6B column (2.6×100 cm)

Cytotoxicity of TP-1 toward SMMC-7721 cells

The potential of TP-1 to inhibit the proliferation of SMMC-7721 cells was determined by the MTT assay (Fig. 2). The results of MTT revealed that 24 h treatment with TP-1 exhibited a dose-dependent inhibitory effect on SMMC-7721 cells compared to control cells, with the concentration increasing ($P<0.05$ or $P<0.01$). At the highest concentration of 100 μg/mL used, TP-1 caused a 69.5 % inhibition. On the other hand, TP-1 did not cause any cytotoxicity to cultured nontumorigenic hepatocyte WRL-68 or PPC cells, indicating a very favorable sensitive profile of TP-1 to HCC SMMC-7721 cells.

Effects of TP-1 on tumor adhesion and invasion of SMMC-7721 cells

To investigate whether TP-1 could inhibit the metastatic growth of HCC, cell adhesion, wound-healing, and migration assays were performed in SMMC-7721 cells. Firstly, we examined the effect of TP-1 on the adhesion of HCC to Matrigel-coated plates. In adhesion assays, TP-1 at an indicated dose significantly and dose-dependently inhibited cell adhesion of SMMC-7721 to the Matrigel-coated substrate compared to the control ($P<0.01$ or $P<0.001$, Fig. 3). Treatment with TP-1 reduced cellular adhesion by approximately 41.7, 58.4, and 68.4 % at concentrations of 25, 50, and 100 μg/mL, respectively, compared with the untreated control.

Next, we employed Transwell migration and wound-healing assay to characterize the cells' migration response to TP-1. In the wound-healing assay, cellular motility of the cells treated with various concentrations of TP-1 for 24 h was much weaker than that of untreated cells, revealing that TP-1 significantly inhibited the motility of SMMC-7721 cells (Fig. 4).

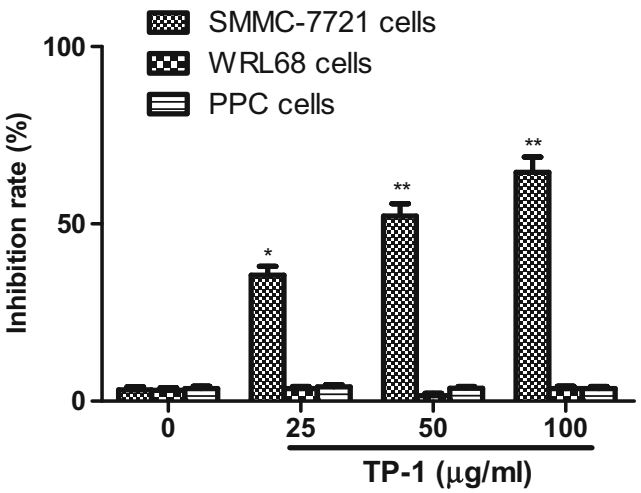

Fig. 2 Cytotoxic effect of TP-1 on SMMC-7721 cells. Data are represented as the mean±SD of at least three independent experiments. $^{*}P<0.05$, $^{**}P<0.01$ compared with untreated cells

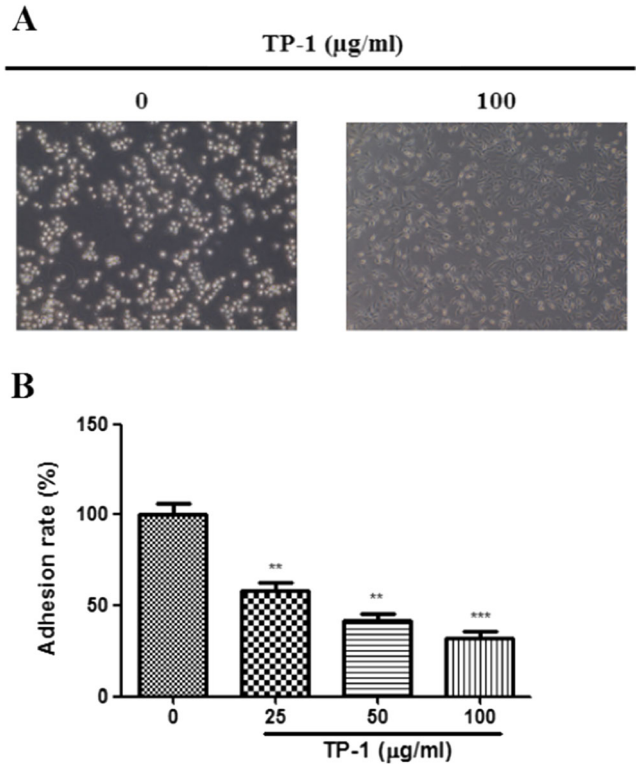

Fig. 3 **a** Representative photo of adhesive SMMC-7721 cells on Matrigel-coated plates treated with or without 100 μg/mL of TP-1. **b** Adhesion rate of SMMC-7721 cells to Matrigel-coated plates in the absence or presence of TP-1 (25, 50, and 100 μg/mL). Data are represented as the mean±SD of at least three independent experiments. $^{**}P<0.01$, $^{***}P<0.001$ compared with untreated cells

Using Transwell chemotaxis migration assay, we found that treatment with TP-1 for 24 h significantly attenuated the migration of SMMC-7721 cells through the Transwell membrane under 10 % FCS attraction compared to vehicle-treated cells ($P<0.05$, $P<0.01$, or $P<0.001$) in a dose-dependent manner, with the inhibition rate of 37.8, 52.0, and 61.9 %, at concentrations of 25, 50, and 100 μg/mL of TP-1, respectively (Fig. 5). All these findings indicated that TP-1 was involved in suppressing both the wound-induced and 10 % FCS-attracted SMMC-7721 cell migration.

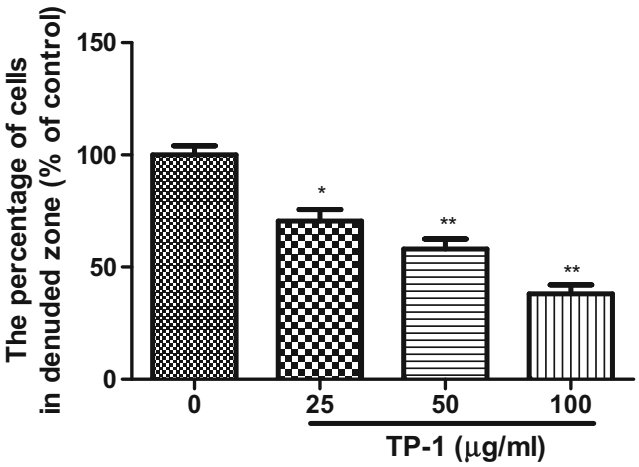

Fig. 4 Effect of TP-1 (0, 25, 50, and 100 μg/mL) on the motility of SMMC-7721 cells in the wound-healing assay. Data are represented as the mean±SD of at least three independent experiments. $^{*}P<0.05$, $^{**}P<0.01$ compared with untreated cells

Effects of TP-1 on the level of AUF-1, AEG-1, and miR-122 in SMMC-7721 cells

Having shown that treatment of SMMC-7721 cells with TP-1 significantly inhibited the cell adhesion, migration, and invasion, we next investigate the underlying mechanisms as to which gene accounted for the TP-1-reduced metastasis in SMMC-7721 cells. Two cancer-promoting genes (AUF-1 and AEG-1) and one cancer-suppressing gene (miR-122) were examined in the present experiment. As seen in Fig. 6, AUF-1 and AEG-1 mRNA and the corresponding protein expression were downregulated in SMMC-7721 cells when treated with TP-1, whereas miR-122 level increased following 24 h exposure to TP-1.

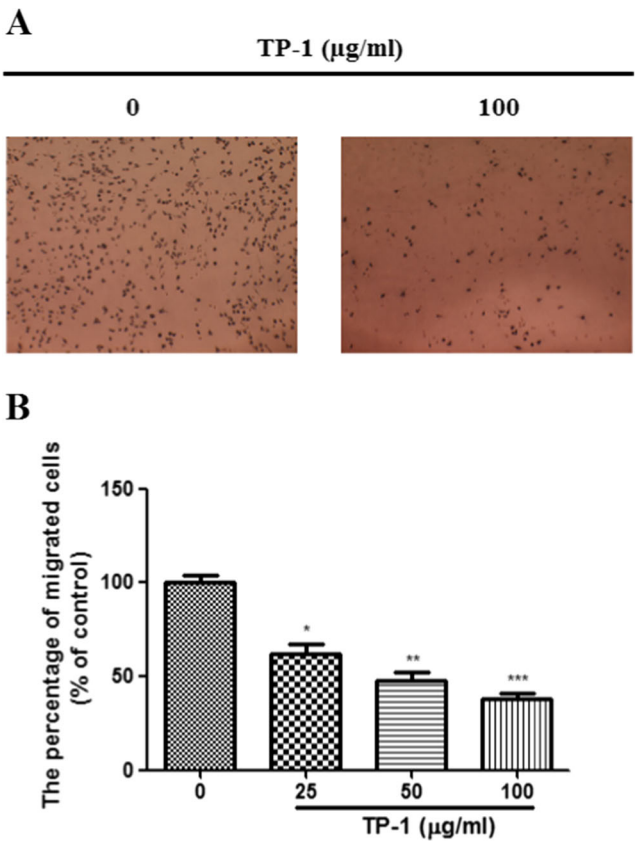

Fig. 5 **a** Representative photo of migrated SMMC-7721 on the underside of the Transwell membrane treated with or without 100 μg/mL of TP-1. **b** Effect of TP-1 (0, 25, 50, and 100 μg/mL) on migration of SMMC-7721 cells in Transwell chemotaxis migration assay. Data are represented as the mean±SD of at least three independent experiments. $^{*}P<0.05$, $^{**}P<0.01$, $^{***}P<0.001$ compared with untreated cells

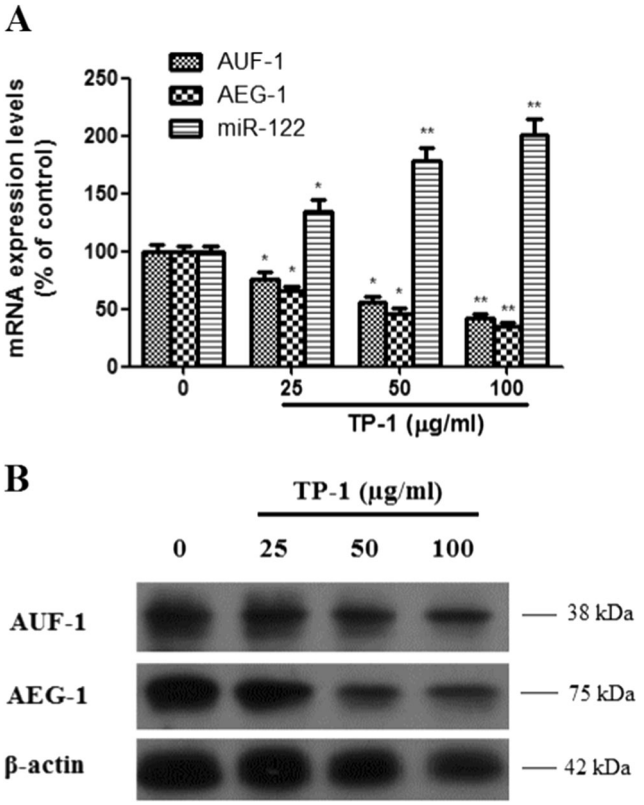

Fig. 6 **a** The mRNA expression of AUF-1, AEG-1, and miR-122 in TP-1-treated SMMC-7721 cells. Data are represented as the mean±SD of at least three independent experiments. $^{*}P<0.05$, $^{**}P<0.01$ compared with untreated cells. **b** The protein expression of AUF-1 and AEG-1 in TP-1-treated SMMC-7721 cells

Effects of TP-1 on E-cadherin and N-cadherin protein expression in SMMC-7721 cells

Since EMT plays a crucial role in progression in the development of invasive cancer cells [19], we assessed the effect of TP-1 on EMT markers in SMMC-7721 cells by Western blotting. TP-1 treatment at three concentrations apparently increased epithelial marker E-cadherin level but decreased the mesenchymal marker N-cadherin expression (Fig. 7).

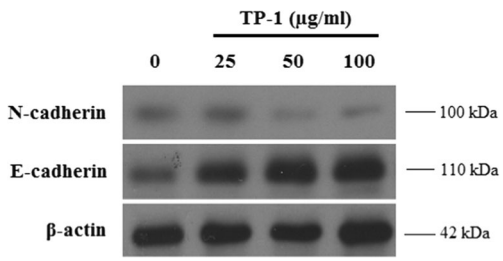

Fig. 7 The protein expression of E-cadherin and N-cadherin in TP-1-treated SMMC-7721 cells

Effects of TP-1 on lung metastasis of SMMC-7721 cells in vivo

To further confirm the antimetastatic effect of TP-1 on in vivo lung metastasis of liver cancer, mouse lung slices were stained with hematoxylin-eosin (H & E) in nude BALB/c mice suffering from an orthotopic implantation of SMMC-7721 tumor tissue. The result of H & E staining of lung tissues in Fig. 8 proved that many metastatic colonies were observed in the lungs of untreated mice, while the lungs of mice treated with TP-1 showed a decrease in the number of lung metastatic nodules, which was statistically significant at the doses of 400 and 800 μg/kg compared with those of the control mice ($P<0.05$). Additionally, the TP-1-treated mice appeared to have no weight loss throughout the treatment, indicating that TP-1 showed little toxicity.

Discussion and conclusions

Metastasis and overgrowth are the most devastating characteristics of highly malignant cancers, and they are related to cancer therapeutic efficacy and prognostic survival [20]. Advances in surgical techniques and systemic therapies are therapeutically useful in the treatment of primary tumors [21]. However, HCC is an aggressive malignancy with poor prognosis and often is diagnosed at the middle or advanced stages [8, 22]. Even in patients undergoing surgical resection, the high incidence of postoperative recurrence and metastasis remains a big challenge for further survival, accounting for the poor long-term survival of HCC [23, 24]. Also, HCC is resistant to most conventional chemotherapeutic agents [25]. Therefore, it is urgent to develop novel agents with low toxicity to normal cells and high efficacy on both HCC growth and metastasis. In the present study, we first investigated the

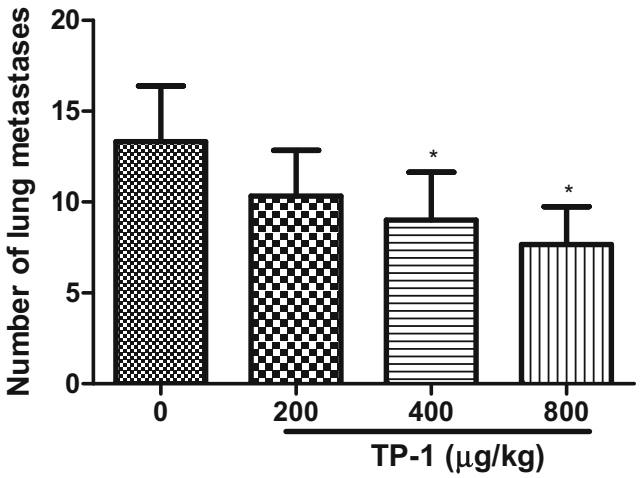

Fig. 8 Number of visible tumors on lung surface of mice treated with TP-1. Data are represented as the mean±SD of six independent experiments. $^{*}P<0.05$ compared with untreated mice

in vitro effect of TP-1, a purified polysaccharide from mushroom Huaier, on cell growth and metastatic potential of HCC SMMC-7721 cells.

The inhibitory effect of TP-1 on the growth of SMMC-7721 cells was determined by the MTT assay. We have provided evidence for the first time that TP-1 exerted a favorable antiproliferative effect on SMMC-7721 cells in vitro. Encouragingly, TP-1 had no toxicity on human liver WRL-68 and PCC cell lines, indicating the potential of TP-1 as an ideal antitumor agent.

The adhesion, migration, and invasiveness of tumor cells represent a set of unique biological properties necessary for the formation of metastases [26, 27]. With the goal of exploring the antimetastatic effects of TP-1 on human HCC cells, cell adhesion, wound-healing, and migration assays were performed in SMMC-7721 cells. We found that TP-1 (25, 50, or 100 μg/mL) dose-dependently inhibited cancer cell adhesion, invasion, and migration of SMMC-7721 cells in vitro. All these findings indicated that TP-1 could prevent the metastatic potential of SMMC-7721 cells in vitro.

According to previous studies, elevated expression of AUF-1 and AEG-1 has been demonstrated to be associated with the progression and invasion of HCC cells [5]. Therefore, we can conclude that decreased AUF-1 and AEG-1 expression would contribute to the inhibition of metastasis of HCC cells. Here, we demonstrated that AUF-1 and AEG-1 were decreased in both transcript and protein levels in SMMC-7721 cells upon TP-1 treatment.

Numerous studies have started to shed light on the importance of miRNA in hepatocarcinogenesis. Among them, miR-122, as a tumor suppressor gene, appears to play an important role in hepatocarcinogenesis, particularly intrahepatic metastasis [28, 29]. There is also evidence that lower expression level of miR-122 is related to the migration and invasion activity of HCC cells [30]. Thus, suppression of miR-122 would facilitate the eradication of HCC growth and metastasis. In the present study, the level of miR-122 in SMMC-7721 cells was increased by TP-1 treatment.

Accumulating evidence indicates that epithelial-mesenchymal transition (EMT) plays an important role during tumorigenesis and metastasis [20]. In aggressive tumors, this process is characterized by reduced expression of epithelial marker (E-cadherin) and increased expression of mesenchymal marker (N-cadherin), which increased tumor cell motility and invasive properties to initiate metastasis [31, 32]. To further understand the antimetastatic mechanism mediated by TP-1, the expression of E-cadherin and N-cadherin was analyzed in SMMC-7721 cells. Western blot results showed that exposure to TP-1 at three concentrations retarded the transformation of SMMC-7721 cells from a typical epithelial phenotype to a spindle-shaped mesenchymal phenotype, as indicated by an upregulation of E-cadherin and a loss of N-cadherin, suggesting that the antimetastatic effect of TP-1 on SMMC-7721 cells was associated with inhibition of EMT.

In agreement with the results of our in vitro model, the inhibitory effect of TP-1 on lung metastasis of liver cancer was further verified in vivo. The number of lung metastatic nodules was significantly inhibited by oral administration of TP-1 at a daily dose of 400 and 800 μg/kg in experimental animals. Additionally, the body weight of the TP-1-treated mice had no difference compared with that of control mice at the end of treatment.

In conclusion, we proved that the inhibition of cell proliferation, adhesion, migration, and motility by TP-1 was achieved not only by reducing the expression of AUF-1, AEG-1, and N-cadherin but also by enhancing miR-122 and E-cadherin expression in a dose-dependent manner. We also found that TP-1 could inhibit lung metastasis of liver cancer in an in vivo murine model, which was consistent with the in vitro findings.

Acknowledgments This research is funded by the National Natural Science Foundation of China (grant no. 81472328); Liver Disease AIDS Foundation of You An Hospital, Capital Medical University (BJYAH-2011-034); National Science and Technology Support Project (2012BAI15B08); and Key Project of National Communicable Disease (2012ZX10002015-002).

Conflicts of interest The authors declare that they have no conflicts of interest concerning this article.

References

1. Zhang CL, Zeng T, Zhao XL, Yu LH, Zhu ZP, Xie KQ. Protective effects of garlic oil on hepatocarcinoma induced by N-nitrosodiethylamine in rats. Int J Biol Sci. 2012;8:363–74.
2. Sporn MB. The war on cancer. Lancet. 1996;347:1377–81.
3. Fidler IJ. Critical factors in the biology of human cancer metastasis: twenty-eighth G.H.A. Clowes memorial award lecture. Cancer Res. 1990;50:6130–8.
4. Arvelo F, Cotte C. Metalloproteinases in tumor progression. Review. Invest Clin. 2006;47:185–205.
5. Yang Y, Kang P, Gao J, Xu C, Wang S, Jin H, et al. AU-binding factor 1 expression was correlated with metadherin expression and progression of hepatocellular carcinoma. Tumour Biol. 2014;35:2747–51.
6. Zheng J, Li C, Wu X, Yang Y, Hao M, Sheng S, et al. Astrocyte elevated gene-1 is a novel biomarker of epithelial–mesenchymal transition and progression of hepatocellular carcinoma in two China regions. Tumour Biol. 2014;35:2265–9.
7. Nakao K, Miyaaki H, Ichikawa T. Antitumor function of microRNA-122 against hepatocellular carcinoma. J Gastroenterol. 2014;49:589–93.
8. Zheng J, Li C, Wu X, Liu M, Sun X, Yang Y, et al. Huaier polysaccharides suppresses hepatocarcinoma MHCC97-H cell metastasis via inactivation of EMT and AEG-1 pathway. Int J Biol Macromol. 2014;64:106–10.
9. Staub AM. Removal of protein—Sevag method. Methods Carbohydr Chem. 1965;5:5–6.

10. Tian J, Che H, Ha D, Wei Y, Zheng S. Characterization and anti-allergic effect of a polysaccharide from the flower buds of Lonicera japonica. Carbohydr Polym. 2012;90:1642–7.
11. Dubois M, Gilles KA, Hamilton JK, Rebers PA, Smith F. Colorimetric method for determination of sugars and related substances. Anal Chem. 1956;28:350–6.
12. Bradford MM. A rapid and sensitive method for the quantitation of microgram quantities of protein utilizing the principle of protein binding. Anal Biochem. 1976;72:248–54.
13. Blumenkrantz N, Asboe-Hansen G. New method for quantitative determination of uronic acids. Anal Biochem. 1973;54:484–9.
14. Mosmann T. Rapid colorimetric assay for cellular growth and survival: application to proliferation and cytotoxicity assays. J Immunol Methods. 1983;65:55–63.
15. Saiki I, Iida J, Murata J, Ogawa R, Nishi N, Sugimura K, et al. Inhibition of the metastasis of murine malignant melanoma by synthetic polymeric peptides containing core sequences of cell-adhesive molecules. Cancer Res. 1989;49:3815–22.
16. Livak KJ, Schmittgen TD. Analysis of relative gene expression data using real-time quantitative PCR and the 2(−Delta Delta C(T)) method. Methods. 2001;25:402–8.
17. Man K, Ng KT, Xu A, Cheng Q, Lo CM, Xiao JW, et al. Suppression of liver tumor growth and metastasis by adiponectin in nude mice through inhibition of tumor angiogenesis and downregulation of Rho kinase/IFN-inducible protein 10/matrix metalloproteinase 9 signaling. Clin Cancer Res. 2010;16:967–77.
18. Sun FX, Tang ZY, Lui KD, Ye SL, Xue Q, Gao DM, et al. Establishment of a metastatic model of human hepatocellular carcinoma in nude mice via orthotopic implantation of histologically intact tissues. Int J Cancer. 1996;66:239–43.
19. Micalizzi DS, Farabaugh SM, Ford HL. Epithelial-mesenchymal transition in cancer: parallels between normal development and tumor progression. J Mammary Gland Biol Neoplasia. 2010;15:117–34.
20. Cai JP, Wu YJ, Li C, Feng MY, Shi QT, Li R, et al. Panax ginseng polysaccharide suppresses metastasis via modulating Twist expression in gastric cancer. Int J Biol Macromol. 2013;57:22–5.
21. Entschladen F, Drell 4th TL, Lang K, Joseph J, Zaenker KS. Tumour-cell migration, invasion, and metastasis: navigation by neurotransmitters. Lancet Oncol. 2004;5:254–8.
22. Ng KT, Guo DY, Cheng Q, Geng W, Ling CC, Li CX, et al. A garlic derivative, S-allylcysteine (SAC), suppresses proliferation and metastasis of hepatocellular carcinoma. PLoS One. 2012;7:e31655.
23. Feng YX, Wang T, Deng YZ, Yang P, Li JJ, Guan DX, et al. Sorafenib suppresses postsurgical recurrence and metastasis of hepatocellular carcinoma in an orthotopic mouse model. Hepatology. 2011;53:483–92.
24. Tang ZY, Ye SL, Liu YK, Qin LX, Sun HC, Ye QH, et al. A decade's studies on metastasis of hepatocellular carcinoma. J Cancer Res Clin Oncol. 2004;130:187–96.
25. Zheng J, Li C, Wu X, Liu M, Sun X, Yang Y, et al. Astrocyte elevated gene-1 (AEG-1) shRNA sensitizes Huaier polysaccharide (HP)-induced anti-metastatic potency via inactivating downstream P13K/Akt pathway as well as augmenting cell-mediated immune response. Tumour Biol. 2014;35:4219–24.
26. Gu Y, Zhu CF, Dai YL, Zhong Q, Sun B. Inhibitory effects of genistein on metastasis of human hepatocellular carcinoma. World J Gastroenterol. 2009;15:4952–7.
27. Rouhi P, Lee SL, Cao Z, Hedlund EM, Jensen LD, Cao Y. Pathological angiogenesis facilitates tumor cell dissemination and metastasis. Cell Cycle. 2010;9:913–7.
28. Köberle V, Kronenberger B, Pleli T, Trojan J, Imelmann E, Peveling-Oberhag J, et al. Serum microRNA-1 and microRNA-122 are prognostic markers in patients with hepatocellular carcinoma. Eur J Cancer. 2013;49:3442–9.
29. Xu J, Zhu X, Wu L, Yang R, Yang Z, Wang Q, et al. MicroRNA-122 suppresses cell proliferation and induces cell apoptosis in hepatocellular carcinoma by directly targeting Wnt/β-catenin pathway. Liver Int. 2012;32:752–60.
30. Tsai WC, Hsu PW, Lai TC, Chau GY, Lin CW, Chen CM, et al. MicroRNA-122, a tumor suppressor microRNA that regulates intrahepatic metastasis of hepatocellular carcinoma. Hepatology. 2009;49:1571–82.
31. Wang L, Alcon A, Yuan H, Ho J, Li QJ, Martins-Green M. Cellular and molecular mechanisms of pomegranate juice-induced anti-metastatic effect on prostate cancer cells. Integr Biol (Camb). 2011;3:742–54.
32. Yoon JH, Choi YJ, Cha SW, Lee SG. Anti-metastatic effects of ginsenoside Rd via inactivation of MAPK signaling and induction of focal adhesion formation. Phytomedicine. 2012;19:284–92.